Electronic Research Archive

ERA, 34(10): 7071–7095.
DOI: 10.3934/era.2026306
Received: 05 June 2026
Revised: 29 July 2026
Accepted: 07 August 2026
Published: 17 August 2026

https://www.aimspress.com/journal/ERA

Research article

Event-triggered adaptive prescribed-time control of a class of uncertain nonlinear systems with time-varying parameters and disturbances

Litong Zhou[1], Ruicheng Zhang[1], Lichao Feng[1,2,*] and Weizheng Liang[1,*]

[1] College of Electrical Engineering, North China University of Science and Technology, Tangshan 063210, China

[2] College of Sciences, North China University of Science and Technology, Tangshan 063210, China

* **Correspondence:** Email: fenglichao@ncst.edu.cn, wzliang1982@126.com.

Abstract: For a class of strict-feedback nonlinear systems involving unknown time-varying parameters and external disturbances, an event-triggered adaptive prescribed-time control method is proposed. First, a prescribed-time adjustment function containing only a single reciprocal term is introduced to unify the multi-stage high-order scaling in conventional prescribed-time backstepping into a single first-order scaling, thereby simplifying the structure of the prescribed-time scaling term and reducing the complexity of the recursive controller design. Second, an adaptive law is developed to adaptively compensate for the effects of unknown time-varying parametric uncertainties, while a radial basis function neural network (RBFNN) is embedded into the backstepping framework to achieve real-time approximation and compensation of external disturbances. Moreover, an event-triggered mechanism is incorporated to operate synchronously with the controller, guaranteeing prescribed-time stability and substantially reducing the number of control updates compared with periodic sampling, thus saving communication and computational resources. Finally, numerical simulations demonstrate that the proposed control strategy achieves prescribed-time convergence and post-prescribed-time practical boundedness, while maintaining satisfactory robustness with significantly fewer control updates.

Keywords: time-varying parameters; uncertain nonlinear systems; prescribed-time stability; adaptive backstepping control; event-triggered control; neural network control

1. Introduction

In recent years, prescribed-time control has become a research hotspot in control theory and engineering applications because its convergence time is independent of both the initial conditions and the control gains. Early control methods mainly focused on asymptotic stability, which features a slow convergence rate and is unsuitable for applications requiring strong real-time performance. Although finite-time control [1] can guarantee that the system reaches equilibrium within a finite time, its convergence time depends on the initial conditions. Fixed-time control [2] decouples the convergence time from the initial conditions but is highly sensitive to design parameters, making parameter tuning difficult. The emergence of prescribed-time control theory [3] achieves convergence within a time that is independent of both the initial conditions and the control parameters, enabling the system to reach equilibrium precisely at a user-specified instant. This lays a solid foundation for the development of highly reliable and real-time control systems.

However, early prescribed-time control methods were mostly based on state scaling or time scaling design [4,5], which often resulted in complicated structures and strong parameter dependence, making unified and simplified controller design difficult. In addition, the prescribed-time control approach that mainly relies on state-scale and time-scale transformations [6] can guarantee convergence before the prescribed time, but its design procedure typically requires multi-level scaling and nested nonlinear terms, leading to a complex control law and a heavy structural complexity. To address this issue, Zhou and Shi [7] proposed a non-scaling prescribed-time stability framework, which achieves consistent convergence performance throughout the entire control process without introducing multiple time-varying scaling functions, thereby reducing implementation complexity. In [8], an adaptive estimation mechanism was introduced, and an adaptive prescribed-time control law was developed for nonlinear systems with parametric uncertainty, together with a new prescribed-time stability theorem. Subsequently, for systems with input delays, Ning et al. [9] extended the prescribed-time framework to time-delay dynamics and performed adaptive prescribed-time stability analysis. Considering engineering scenarios with state constraints, Liu et al. [10] incorporated boundary-handling techniques into adaptive prescribed-time control and proposed a state-prescribed control strategy. Recent studies have further extended prescribed-time control to more complex nonlinear systems. Zhang et al. [11] investigated prescribed-time adaptive fuzzy optimal control for nonlinear systems, whereas Zhang et al. [12] developed a predefined-time adaptive fuzzy control scheme for nonlinear systems with output hysteresis. Feng et al. [13] proposed an improved time-varying feedback approach for prescribed-time stabilization of nonlinear systems subject to uncertainties and disturbances. In addition, prescribed-time stability criteria for nonlinear impulsive piecewise systems and impulsive piecewise-smooth differential systems, together with their synchronization and network applications, were established in [14,15]. These studies have enriched the theoretical framework and application scope of prescribed-time control.

Nevertheless, most existing results do not simultaneously consider unknown time-varying parametric uncertainties, external disturbances, and resource-constrained event-triggered implementation. However, when the parameters are time-varying and uncertain, such cases are of great significance in practical applications such as missile guidance, cooperative unmanned aerial vehicle (UAV) control, and spacecraft docking. Therefore, investigating prescribed-time control for uncertain nonlinear systems with time-varying parameter uncertainty is of particular importance. In practical engineering, system operation is also often accompanied by unknown external disturbances, which may even cause equipment damage in severe cases. Although neural-network control approaches [16] can approximate and compensate for unknown nonlinearities and disturbances online, relatively few prescribed-time control results simultaneously address time-varying parametric uncertainties, external disturbances, and event-triggered implementation. Despite the rich achievements in handling model uncertainty, time delays, and state constraints, research on prescribed-time control for uncertain nonlinear systems that simultaneously contain unknown external disturbances and time-varying parametric uncertainty remains relatively limited.

With the rapid development of networked control systems and the Internet of Things (IoT), maintaining prescribed-time convergence under limited bandwidth and computational resources has become a new challenge. Event-triggered mechanisms have attracted increasing attention because they can significantly reduce control updates and communication costs while satisfying performance requirements. Related intelligent event-triggered control schemes have also been reported. Li et al. [17] developed an adaptive fuzzy event-triggered command-filtered controller for nonlinear time-delay systems, while Li et al. [18] proposed a neural-network-approximation-based adaptive periodic event-triggered output-feedback controller for switched nonlinear systems. These studies demonstrate the effectiveness of combining adaptive approximation techniques with event-triggered implementation. However, they do not address prescribed-time stabilization of strict-feedback nonlinear systems simultaneously affected by unknown time-varying parametric uncertainties and external disturbances. Ning et al. [19] introduced event-triggered strategies into prescribed-time control of nonlinear uncertain systems and established general convergence criteria. Furthermore, Ning et al. [20] designed a new dynamic event-triggered mechanism and collaboratively developed a prescribed-time controller, which effectively reduces the triggering frequency and alleviates the communication burden of networked systems. In summary, although existing studies have achieved notable progress in event-triggered prescribed-time control, further research is still required to address uncertain nonlinear systems subject to both time-varying parameters and external disturbances under resource constraints.

Based on the above analysis, the main contributions of this study can be summarized as follows:

1) For strict-feedback nonlinear systems with unknown time-varying parametric uncertainties, a single-reciprocal prescribed-time adjustment function is incorporated into the adaptive backstepping design. Compared with multi-layer scaling-based prescribed-time methods, the proposed design involves only one first-order time-varying scaling function, which simplifies the recursive controller structure and reduces the structural complexity of the controller design. Moreover, the adaptive law is used to compensate for the effects of time-varying parametric uncertainties rather than to identify their exact trajectories.

2) An RBFNN is employed to approximate and compensate for the unknown external disturbance online. The NN weight estimate is updated according to the closed-loop error signal, and the NN output is directly embedded into the control input as a compensation term. In this way, the exact value of the external disturbance is not required in the controller, and the influence of the RBFNN approximation error is incorporated into the Lyapunov stability analysis.

3) An event-triggered mechanism is incorporated into the prescribed-time adaptive backstepping framework. Compared with time-triggered implementation, the proposed event-triggered strategy significantly reduces the number of control input updates while maintaining prescribed-time convergence. Unlike some existing event-triggered prescribed-time methods that mainly focus on time-varying parametric uncertainties, the proposed framework further includes RBFNN-based compensation for unknown external disturbances.

2. Problem description and preliminaries

2.1. Problem formulation

Consider the following class of strict-feedback nonlinear systems with uncertain time-varying parameters and external disturbances:

$$\begin{aligned} \dot{x}_i &= x_{i+1} + \theta_i^T(t) f_i(\bar{x}_i), i = 1, \dots, n-1 \\ \dot{x}_n &= u + \theta_n^T(t) f_n(\bar{x}_n) + w(t) \end{aligned}, \tag{1}$$

where $\bar{x}_i = [x_1, \dots, x_i]^T \in R^i$ is the system state; $\theta_i(t) \in R^r$ is the uncertain time-varying bounded parameters vector; $f_i(\cdot): R^i \to R^r$ are the known continuous functions with $f_i(0) = 0, i = 1,2, \dots, n$. u is control input, $w(t)$ represents bounded continuous disturbances.

Assumption 1: The unknown time-varying parameter vectors are continuously differentiable and bounded. There exist unknown positive constants

$$\begin{aligned} \|\theta_i(t)\| &\le \bar{\theta}_i, \\ \|\dot{\theta}_i(t)\| &\le \bar{\theta}_{di}, i = 1, \dots, n. \end{aligned} \tag{2}$$

This assumption is reasonable because physical parameters in practical systems, such as resistance, friction coefficients, aerodynamic coefficients, load variations, and environmental parameters, usually vary within finite ranges and cannot change infinitely fast due to physical constraints, actuator bandwidth, and sensor limitations.

Remark 1: For system (1) with uncertain time-invariant parameters and without external disturbances, the adaptive event-triggered finite-time control problem has been investigated in [21], where a global fast finite-time stable scheme was developed. However, the co-designed controller and event-triggering mechanism can only guarantee finite-time convergence, and the settling time still depends on the initial conditions rather than being prescribed a priori. In many practical applications, such as missile precision strike, cooperative UAV missions, and autonomous spacecraft rendezvous and docking, it is more desirable to achieve prescribed-time convergence that is independent of both the initial conditions and control gains. Motivated by this, the present work investigates the prescribed-time control problem for a class of strict-feedback nonlinear systems with uncertain time-varying parameters and unknown external disturbances and develops an adaptive event-triggered prescribed-time control scheme that ensures user-specified convergence while reducing communication and structural complexity.

The control objective is to design an event-triggered adaptive prescribed-time controller such that the system states converge to the origin at the prescribed instant T_p and remain within a bounded neighborhood of the origin after T_p, while excluding Zeno behavior.

2.2. Preliminaries

Definition 1 ([19]): A continuous function is called a prescribed-time adjustment function (PTA function) if it satisfies

$$\mu(t) > 0,\ \forall t \in [0,\mathrm{T}_p), \\ \lim_{t\to T_p^-}(T_p - t)\mu(t) = o. \tag{3}$$

where o is a positive constant or $+\infty$.

Lemma 1 ([20])**:** For any nonnegative differentiable functions $V_1(t)$ and $V_2(t)$, a positive continuous function $\sigma(t)$, and a constant $p \in (0,1)$, suppose that

$$\lim_{t\to T_p^-}(T_p - t)^p\mu(t)\sigma(t) = \bar{\sigma} < +\infty \\ V(t) = V_1(t) + V_2(t),\ t \in [0,\mathrm{T}_p), \\ \dot{V}(t) \le -c\mu(t)V_1(t) + \varepsilon\mu(t)\sigma(t), \tag{4}$$

where $\mu(t)$ is a PTA function, $c > 0, \varepsilon > 0$, and $\bar{\sigma} \ge 0$ are constants. Then, $V(t)$ is bounded on $[0,\mathrm{T}_p)$, and $\lim_{t\to T_p^-} V_1(t) = 0$.

Corollary 1: Consider a nonnegative Lyapunov function $V(t)$ satisfying

$$V(t) = V_1(t) + V_2(t),\ t \in [0,\mathrm{T}_p), \tag{5}$$

where $V_1(t) \ge 0$ and $V_2(t) \ge 0$. If

$$\dot{V}(t) \le -c\mu(t)V_1(t) + \varepsilon\mu(t)\sigma(t) + \eta, \tag{6}$$

where $c > 0, \varepsilon > 0, \eta > 0$ and $\sigma(t)$ satisfies

$$\lim_{t\to T_p^-}(T_p - t)^p\mu(t)\sigma(t) = \bar{\sigma} < +\infty, p \in (0,1), \tag{7}$$

then $V(t)$ is bounded on $[0,\mathrm{T}_p)$, and $\lim_{t\to T_p^-} V_1(t) = 0$.

Proof: By applying the **Gronwall Lemma** inequality to (6), one obtains

$$V(t) \le V(0)e^{-c\int_0^t \mu(s)ds} + e^{-c\int_0^t \mu(s)ds}\int_0^t (c\mu(s)V_2 + n\mu(s)d\sigma(s) + \eta)e^{c\int_0^s \mu(\tau)d\tau}ds, \tag{8}$$

according to **Definition 1**, for the PTA function $\mu(t)$, it holds that $\lim_{t\to T_P^-}\int_0^t \mu(s)ds = +\infty$. Using this fact together with **L'Hôpital's rule** yields

$$\begin{aligned}\lim_{t\to T_P^-} V(t) &= \lim_{t\to T_P^-}(V_1 + V_2) \\ &\le \lim_{t\to T_P^-}\frac{\int_0^t (c\mu(s)V_2 + \varepsilon\mu(s)d\sigma(s) + \eta)e^{-c\int_0^S \mu(\tau)d\tau}ds}{e^{c\int_0^t \mu(s)ds}} \\ &= \lim_{t\to T_P^-}\left(V_2 + \frac{\varepsilon d\sigma(s)}{c} + \frac{\eta}{c\mu(t)}\right) \\ &= \lim_{t\to T_P^-}\left(V_2 + \frac{\varepsilon d\sigma(s)}{c}\right)\end{aligned}, \tag{9}$$

where we have used $\lim_{t\to T_P^-}\sigma(t) = 0$. Therefore, combining with (8), it follows that

$$\lim_{t\to T_P^-} V(t) = \lim_{t\to T_P^-}(V_1 + V_2) \le \lim_{t\to T_P^-} V_2. \tag{10}$$

Therefore, $\lim_{t\to T_P^-} V_1(t) = 0$.

Lemma 2 ([22])**:** For any functions $x \ge 0, y \ge 0$ and any positive constants $p > 1, q > 1, \frac{1}{p} + \frac{1}{q} = 1$, the following inequality holds:

$$xy \le \frac{x^p}{p} + \frac{y^q}{q}. \tag{11}$$

Lemma 3 ([23])**:** For any $\rho > 0$ and any $z \in R$, the following inequality holds:

$$0 \le |z| - z\, tanh(\frac{z}{\rho}) \le 0.2785\rho. \tag{12}$$

2.3. Radial basis function neural network

The radial basis function neural network (RBFNN) is a type of feedforward neural network constructed with nonlinear radial basis functions. It is widely used for approximating continuous functions and can be expressed as

$$F(z) = W^{*T}\Omega(z) + \varepsilon(z), \tag{13}$$

where ε is the approximation error satisfying $|\varepsilon(z)| \le \bar{\varepsilon}$, with $\bar{\varepsilon} > 0$ being a constant bound. The optimal weight W^* vector is defined as

$$W^* = argmin\{sup|F(z) - \widehat{W}^T\Omega(z)|\}. \tag{14}$$

Let $\widehat{W}$ be the estimate of W^*, and $\Omega(z) = [\Omega_1(z), \Omega_2(z), \dots, \Omega_i(z)]^T$ be the vector of basis functions, which are designed as

$$\Omega_i(z) = exp\left[\frac{-(z-\varsigma_i)^T(z-\varsigma_i)}{\kappa_i^2}\right], \tag{15}$$

where ς_i denotes the center of the i -th basis function, and κ_i is a positive design parameter. In this paper, the RBFNN input is selected as $z = x_n$, and the unknown external disturbance $w(t)$ is approximated by the RBFNN as

$$w(t) = W^{*T}\Omega(x_n) + \varepsilon(x_n, t). \tag{16}$$

The NN output is written as

$$\widehat{w}(t) = \widehat{W}^T\Omega(x_n). \tag{17}$$

Different from offline-trained neural networks, the weight estimate $\widehat{W}$ is updated online by the adaptive law during the closed-loop operation. Therefore, the exact value of $w(t)$ is not required in the controller.

3. Main results

In this section, a prescribed-time controller design is developed by integrating a prescribed-time adjustment function with an event-triggered mechanism within a backstepping framework. The proposed scheme not only significantly reduces communication resources but also eliminates the dependence of the system's convergence time on initial conditions and control parameters.

3.1. Virtual control law design

To simplify the subsequent analysis, the following state transformation is applied to system (1):

$$\begin{aligned} &\xi_1 = \mu(t)\lambda_1,\ \lambda_1 = x_1,\\ &\xi_i = \mu(t)\lambda_i,\ \lambda_i = x_i - \alpha_{i-1},\ i = 2, \dots, n, \end{aligned} \tag{18}$$

where $\lambda_i (i = 1,\dots,n)$ denotes the recursive error variable introduced in the backstepping design. Specifically, $\lambda_1 = x_1$ represents the first recursive error variable, while $\lambda_i = x_i - \alpha_{i-1} (i = 2,\dots,n)$ represents the error between the actual state x_i and the virtual controller α_{i-1} designed at the previous step, and $\mu(t)$ is the prescribed-time adjustment function (PTA function) defined in Definition 1. To reduce the structural complexity of the system, the time-varying function $\mu(t)$ is chosen as

$$\begin{aligned} &\mu(t) = \frac{1}{T_p - t}, \quad t \in [0, T_p),\\ &\mu(t) = \eta, \quad t \in [T_p, +\infty), \end{aligned} \tag{19}$$

where $\eta > 0$ is a constant.

The virtual control laws and adaptive laws are constructed in accordance with the backstepping design procedure, which consists of n steps.

Step 1: According to (1) and (18),

$$\dot{\xi}_1 = \mu(\alpha_1 + \theta_1^T(t) f_1) + \xi_2 + \mu\xi_1. \tag{20}$$

On this basis, the Lyapunov function is constructed as follows:

$$V_1 = \frac{1}{2}\xi_1^2 + \frac{1}{2}\tilde{d}^2, \tag{21}$$

where $\tilde{d} = d - \hat{d}$ is the estimation error of the unknown function $d = \sup_{t\geq 0}\left\|\theta_1(t), \ \dots, \theta_n(t)\right\|$, and $\hat{d}$ is its estimate.

Then, from (20) and (21)

$$\dot{V}_1 = \mu\xi_1(\alpha_1 + \vartheta_1^T(t)\phi_1 + \xi_1) + \xi_1\xi_2 - \tilde{d}\dot{\hat{d}}, \tag{22}$$

where $\vartheta_1(t) = \theta_1(t)$ and $\phi_1 = f_1$ according to **Lemma 2** and (12),

$$\mu\xi_1\vartheta_1^T(t)\phi_1 \leq \frac{\mu d \xi_1^2 \|\phi_1\|^2}{\sqrt{\xi_1^2\|\phi_1\|^2 + \sigma^2(t)}} + \mu d\sigma(t), \tag{23}$$

where $\sigma(t)=\frac{1}{\mu(t)}=T_p-t$.

From (22) and (23), the virtual control law α_1 can be designed as

$$\alpha_1=-c_1\xi_1-\frac{\hat{d}\xi_1\|\phi_1\|^2}{\sqrt{\xi_1^2\|\phi_1\|^2+\sigma^2(t)}}-\xi_1, \tag{24}$$

where $c_1>n$ is a design parameter.

Substituting (24) into (22) and (23) yields

$$\dot{V}_1\leq -c_1\mu\xi_1^2+\tilde{d}^T\left(\tau_1-\dot{\hat{d}}\right)+\mu d\sigma(t)+\xi_1\xi_2, \tag{25}$$

where $\tau_1=\frac{\mu\xi_1^2\|\phi_1\|^2}{\sqrt{\xi_1^2\|\phi_1\|^2+\sigma^2(t)}}$ is a smooth function on $[0,T_p)$.

Step 2: According to (1) and (18),

$$\dot{\xi}_2=\mu\left(\alpha_2+\vartheta_2^T(t)\phi_2-\frac{\partial\alpha_1}{\partial\hat{d}}\dot{\hat{d}}-\frac{\partial\alpha_1}{\partial x_1}x_2-\frac{\partial\alpha_1}{\partial t}\right)+\xi_3+\mu\xi_2, \tag{26}$$

Next, choose the Lyapunov function $V_2=V_1+\frac{1}{2}\xi_2^2$ that yields

$$\begin{aligned}\dot{V}_2\leq{}& -c_1\mu\xi_1^2+\tilde{d}^T\left(\tau_1-\dot{\hat{d}}\right)+\mu d\sigma(t)+\xi_1\xi_2\\ &+\mu\xi_2\left(\alpha_2+\vartheta_2^T(t)\phi_2-\frac{\partial\alpha_1}{\partial\hat{d}}\dot{\hat{d}}-\frac{\partial\alpha_1}{\partial x_1}x_2-\frac{\partial\alpha_1}{\partial t}\right)+\xi_2\xi_3+\mu\xi_2^2,\end{aligned} \tag{27}$$

according to **Lemma 2** and (27),

$$\mu\xi_2\vartheta_2^T(t)\phi_2\leq\frac{\mu d\xi_2^2\|\phi_2\|^2}{\sqrt{\xi_2^2\|\phi_2\|^2+\sigma^2(t)}}+\mu d\sigma(t), \tag{28}$$

from (27) and (28), the virtual control law α_2 can be designed as

$$\begin{aligned}\alpha_2={}&-c_2\xi_2-\frac{\xi_1}{\mu}-\frac{\hat{d}\xi_2\|\phi_2\|^2}{\sqrt{\xi_2^2\|\phi_2\|^2+\sigma^2(t)}}\\ &+\frac{\partial\alpha_1}{\partial\hat{d}}\tau_2+\frac{\partial\alpha_1}{\partial x_1}x_2+\frac{\partial\alpha_1}{\partial t}-\xi_2\end{aligned}, \tag{29}$$

where $c_2>n-1$ is a design parameter, and $\tau_2=\tau_1+\frac{\mu\xi_2^2\|\phi_2\|^2}{\sqrt{\xi_2^2\|\phi_2\|^2+\sigma^2(t)}}$ is a smooth function on $[0,T_p)$.

Substituting (29) into (27) and (28) yields

$$\begin{aligned}\dot{V}_2\leq{}&-\mu\textstyle\sum_{j=1}^2 c_j\,\xi_j^2+\tilde{d}^T\left(\tau_2-\dot{\hat{d}}\right)+2\mu d\sigma(t)\\ &+\mu\frac{\partial\alpha_1}{\partial\hat{d}}\xi_2\left(\tau_2-\dot{\hat{d}}\right)+\xi_2\xi_3\end{aligned}. \tag{30}$$

Step i $(i=3,\ldots,n-1)$**:** According to (1) and (18),

$$\dot{\xi}_i=\mu\left(\alpha_i+\vartheta_i^T(t)\phi_i-\frac{\partial\alpha_{i-1}}{\partial\hat{d}}\dot{\hat{d}}-\sum_{j=1}^{i-1}\frac{\partial\alpha_{i-1}}{\partial x_j}x_{j+1}-\frac{\partial\alpha_{i-1}}{\partial t}\right)+\xi_{i+1}+\mu\xi_i, \tag{31}$$

where $\vartheta_i^T=[\theta_i^T,\ldots,\theta_1^T]$ and $\phi_i^T=\left[f_i,-\frac{\partial\alpha_{i-1}}{\partial x_{i-1}}f_{i-1},\ldots,-\frac{\partial\alpha_{i-1}}{\partial x_1}f_1\right]$.

Next, choose the Lyapunov function $V_i=V_{i-1}+\frac{1}{2}\xi_i^2$. Using Steps 1 and 2, and proceeding recursively, the time derivative of V_i can be obtained as

$$\begin{aligned}\dot{V}_i\le&-\mu\sum_{j=1}^{i-1}c_j\xi_j^2+\tilde{d}^T\left(\tau_{i-1}-\dot{\hat{d}}\right)+(i-1)\mu d\sigma(t)\\&+\xi_{i-1}\xi_i+\xi_i\xi_{i+1}+\mu\sum_{j=2}^{i-1}\frac{\partial\alpha_{j-1}}{\partial\hat{d}}\xi_j\left(\tau_{i-1}-\dot{\hat{d}}\right)\\&+\mu\xi_i\left(\alpha_i-\frac{\partial\alpha_{i-1}}{\partial\hat{d}}\dot{\hat{d}}-\sum_{j=1}^{i-1}\frac{\partial\alpha_{i-1}}{\partial x_j}x_{j+1}+\vartheta_i^T(t)\phi_i-\frac{\partial\alpha_{i-1}}{\partial t}\right)+\mu\xi_i^2\end{aligned}, \tag{32}$$

where $c_j>n-j+1$ is a design parameter. According to **Lemma 2** and (32),

$$\mu\xi_i\vartheta_i^T(t)\phi_i\le\frac{\mu d\xi_i^2\|\phi_i\|^2}{\sqrt{\xi_i^2\|\phi_i\|^2+\sigma^2(t)}}+\mu d\sigma(t), \tag{33}$$

from (32) and (33), the virtual control law α_i can be designed as

$$\begin{aligned}\alpha_i=&-c_i\xi_i-\frac{\xi_{i-1}}{\mu}-\frac{\hat{d}\xi_i\|\phi_i\|^2}{\sqrt{\xi_i^2\|\phi_i\|^2+\sigma^2(t)}}+\frac{\partial\alpha_{i-1}}{\partial\hat{d}}\tau_i\\&+\sum_{j=1}^{i-1}\frac{\partial\alpha_{i-1}}{\partial x_j}x_{j+1}+\frac{\partial\alpha_{j-1}}{\partial t}-\xi_i+\frac{\xi_i\|\phi_i\|^2}{\sqrt{\xi_i^2\|\phi_i\|^2+\sigma^2(t)}}\sum_{j=2}^{i-1}\frac{\partial\alpha_{j-1}}{\partial\hat{d}}\xi_j,\end{aligned} \tag{34}$$

where $c_i>n-i+1$ is a design parameter, $\tau_i=\tau_{i-1}+\frac{\mu\xi_i^2\|\phi_i\|^2}{\sqrt{\xi_i^2\|\phi_i\|^2+\sigma^2(t)}}$ is a smooth function on $[0,T_p)$.

Substituting (34) into (32) and (33) yields

$$\begin{aligned}\dot{V}_i\le&-\mu\sum_{j=1}^{i}c_j\xi_j^2+\tilde{d}^T\left(\tau_i-\dot{\hat{d}}\right)+i\mu d\sigma(t)\\&+\mu\sum_{j=2}^{i}\frac{\partial\alpha_{j-1}}{\partial\hat{d}}\xi_j\left(\tau_i-\dot{\hat{d}}\right)+\xi_i\xi_{i+1}.\end{aligned} \tag{35}$$

Step n**:** Since the n -th subsystem contains an external disturbance $w(t)$, an RBFNN is employed to approximate $w(t)$. Choose the Lyapunov function

$$V_n=V_{n-1}+\frac{1}{2}\xi_n^2+\frac{1}{2}\delta^{-1}\widetilde{W}^2, \tag{36}$$

where $\widetilde{W}=W^*-\widehat{W}$, δ is the adaptive gain with $\delta>0$.

Next, (36) yields

$$\dot{V}_n \leq -\mu \sum_{j=1}^{n-1} c_j \xi_j^2 + \tilde{d}^T \left(\tau_n - \dot{\hat{d}}\right) + n\mu d\sigma(t)$$
$$+\mu \sum_{j=2}^{n-1} \frac{\partial \alpha_{j-1}}{\partial \hat{d}} \xi_j \left(\tau_n - \dot{\hat{d}}\right) + \mu \xi_n (u - \alpha_n + w(t)) - \delta^{-1} \widetilde{W}^T \dot{\widehat{W}}, \tag{37}$$

where $c_n > 1$ is a design parameter, $\tau_n = \tau_{n-1} + \frac{\mu \xi_n^2 \|\phi_n\|^2}{\sqrt{\xi_n^2 \|\phi_n\|^2 + \sigma^2(t)}}$, α_n is designed as follows:

$$\alpha_n = -c_n \xi_n - \frac{\xi_{n-1}}{\mu} - \frac{\hat{d} \xi_n \|\phi_n\|^2}{\sqrt{\xi_n^2 \|\phi_n\|^2 + \sigma^2(t)}} + \frac{\partial \alpha_{n-1}}{\partial \hat{d}} \tau_n + \sum_{j=1}^{n-1} \frac{\partial \alpha_{n-1}}{\partial x_j} x_{j+1} + \frac{\partial \alpha_{n-1}}{\partial t} - \xi_n$$
$$+ \frac{\xi_n \|\phi_n\|^2}{\sqrt{\xi_n^2 \|\phi_n\|^2 + \sigma^2(t)}} \sum_{j=2}^{n-1} \frac{\partial \alpha_{j-1}}{\partial \hat{d}} \xi_j . \tag{38}$$

Remark 2: Early prescribed-time control methods, such as the time-varying feedback design in [3], usually rely on time-varying gains or scaling-type transformations to achieve convergence at a user-specified time. In traditional prescribed-time backstepping designs, multi-layer time-varying scaling functions are often employed to construct prescribed-time gains. Although these methods can achieve prescribed-time convergence, the repeated use of multi-layer scaling functions and high-order time-varying terms may lead to a complicated recursive controller structure and increase the structural complexity of the controller design. For example, some scaling-based prescribed-time designs involve high-order time-varying scaling terms such as $\mu(t) = T_p/(T_p - t)^m, m \geq 2$. In contrast, the prescribed-time adjustment function used in this paper is chosen as $\mu(t) = 1/(T_p - t)$, which contains only a single first-order reciprocal term. Therefore, only one time-varying scaling function is involved throughout the whole backstepping design. This avoids the repeated construction of multi-layer prescribed-time scaling functions and high-order scaling terms, thereby simplifying the recursive controller structure and reducing the structural complexity of the controller design while preserving the prescribed-time regulation capability. A simple structural comparison is given in Table 1.

Table 1. Structural comparison of prescribed-time adjustment functions.

Method	**PTA function structure**	**Number of PTA functions**	**Scaling order**	**Structural complexity**
Scaling-based prescribed-time methods	Multi-layer scaling functions	Multiple	High-order	Relatively high
Proposed method	Single reciprocal function $\mu(t) = 1/(T_p - t)$	1	First-order	Relatively low

3.2. Event-triggered controller design

In this subsection, the event-triggered mechanism, controller, and adaptive laws are jointly designed, whose explicit forms are given as follows:

$$\begin{cases} u(t) = \upsilon(t_k),\ t \in t_k, t_{k+1}) \\ t_{k+1} = inf\{t > t_k |\ |E(t)| \geq \omega_1\, tanh|u(t)| + \omega_2\}, \end{cases} \tag{39}$$

$$\begin{cases} \upsilon(t) = \alpha_n - \bar{\gamma} - \widehat{W}^T \Omega(\xi_n) \\ \dot{\widehat{W}} = \delta\left(\Omega\mu\xi_n - \beta\widehat{W}\right) \end{cases} \\ \dot{\hat{d}} = \begin{cases} \tau_n, 0 \leq t < T_p \\ 0, t \geq T_p \end{cases}, \tag{40}$$

where $u(t) = \upsilon(t_k)$ is the control input, and $E(t) = \upsilon(t) - u(t)$ denotes the event-triggering error. Moreover, $\bar{\gamma} = \gamma\, tanh\left(\frac{\gamma\mu\xi_n}{k_\gamma}\right)$ is a smooth bounded compensation term, $\gamma > \omega_1 + \omega_2$, and $\gamma, \omega_1, \omega_2, \beta, k_\gamma$ are positive design parameters. The adaptive law in (40) is derived from the Lyapunov stability analysis. The derivative of the final Lyapunov function contains the term $\tilde{d}(\tau_n - \dot{\hat{d}})$; therefore, $\dot{\hat{d}} = \tau_n$ is selected to eliminate this coupling term. It should be noted that $\hat{d}$ estimates an upper-bound-related constant rather than the exact trajectories of the time-varying parameters. Then, it can be seen from (40) that the NN weight estimate $\widehat{W}(t)$ is adjusted online according to the closed-loop error signal ξ_n. Meanwhile, the NN output $\widehat{W}(t)\Omega$ is included in the controller to compensate for the unknown external disturbance. Thus, the RBFNN-based online approximation and compensation are realized through the adaptive weight update and the compensation term in the control input.

When the triggering condition (39) is satisfied, the control input $u(t)$ is updated as $u(t) = \upsilon(t_k)$, and this value is held until the next triggering instant.

For any $t \in t_k, t_{k+1})$, using the triggering condition, one obtains

$$\begin{aligned} |\upsilon - u| &< \omega_1\, tanh|u(t)| + \omega_2 \\ &< \omega_1 + \omega_2. \end{aligned} \tag{41}$$

Therefore, it follows that

$$u(t) = \upsilon(t) - (\omega_1 + \omega_2)\iota(t), \tag{42}$$

where $\iota(t)$ is a continuous function satisfying $|\iota(t)| < 1$.

$$\begin{aligned} \dot{V}_n \leq -\mu \textstyle\sum_{j=1}^{n-1} c_j\, \xi_j^2 + \mu\xi_n(u - \alpha_n + w(t)) - \widetilde{W}^T(\Omega\mu\xi_n - \beta\widehat{W}) \leq -\mu \textstyle\sum_{j=1}^{n} c_j\, \xi_j^2 \\ + n\mu d\sigma(t) + \mu\xi_n(-\bar{\gamma} - \widehat{W}^T\Omega(\xi_n) - (\omega_1 + \omega_2)\iota(t) + W^{*\,T}\Omega(\xi_n) + \varepsilon) \\ -\widetilde{W}^T(\Omega\mu\xi_n - \beta\widehat{W}) \leq -\mu \textstyle\sum_{j=1}^{n} c_j\, \xi_j^2 + n\mu d\sigma(t) + \\ \mu\xi_n(-\bar{\gamma} - (\omega_1 + \omega_2)\iota(t) + \widetilde{W}^{\,T}\Omega(\xi_n) + \varepsilon) - \widetilde{W}^T(\Omega\mu\xi_n - \beta\widehat{W}) \\ \leq -\mu \textstyle\sum_{j=1}^{n} c_j\, \xi_j^2 + n\mu d\sigma(t) - \mu\xi_n(\bar{\gamma} + (\omega_1 + \omega_2)\iota(t)) + \mu\xi_n\varepsilon + \beta\widetilde{W}^T\left(W^* - \widetilde{W}\right) \\ \leq -\mu \textstyle\sum_{j=1}^{n} c_j\, \xi_j^2 + n\mu d\sigma(t) - \mu\xi_n((\omega_1 + \omega_2)\iota(t) + \gamma\, tanh(\frac{\gamma\mu\xi_n}{k_\gamma})) \\ + \mu\|\xi_n\|\|\varepsilon\| + \beta\left\|\widetilde{W}\right\|^T(\bar{W} - \left\|\widetilde{W}\right\|). \end{aligned} \tag{43}$$

By substituting (39) and (40),

$$
\begin{aligned}
&\mu\xi_n\left((\omega_1+\omega_2)\iota(t)+\gamma\tanh\left(\frac{\gamma\mu\xi_n}{k_\gamma}\right)\right)\\
&\quad\le-\left(|\mu\xi_n(\omega_1+\omega_2)|-\gamma\mu\xi_n\tanh\left(\frac{\gamma\mu\xi_n}{k_\gamma}\right)\right)\\
&\quad\le-\left(|\mu\xi_n|-\gamma\mu\xi_n\tanh\left(\frac{\gamma\mu\xi_n}{k_\gamma}\right)\right)\\
&\quad\le-0.2785k_\gamma.
\end{aligned}
\tag{44}
$$

By applying **Lemma 3**,

$$\|\xi_n\|\|\varepsilon\|\le\frac{c_n}{2}\|\xi_n\|^2+\frac{1}{2c_n}\|\varepsilon\|^2. \tag{45}$$

Next, by applying **Lemma 2**,

$$\beta\left\|\widetilde{W}\right\|^T\bar{W}\le\beta\left(\frac{1}{2}\left\|\widetilde{W}\right\|^2+\frac{1}{2}\bar{W}^2\right). \tag{46}$$

Finally, from (43)–(46), it follows that

$$\dot{V}_n\le-c\mu\chi_1+n\mu d\sigma(t)+0.2785k_\gamma+\frac{1}{2}\beta_2\bar{W}^2+\frac{1}{2c_n}\|\varepsilon\|^2, \tag{47}$$

where $c=2\,min\{c_1,\ldots,c_n\},\chi_1=\sum_{j=1}^{n}\xi_j^2$.

3.3. Stability analysis

Theorem 1: For the strict-feedback nonlinear system (1) with unknown time-varying parameters and external disturbances, the event-triggered controller and adaptive laws in (39) and (40) guarantee prescribed-time convergence at T_p, post-prescribed-time practical boundedness, and exclusion of Zeno behavior.

Proof: Rewrite (47) as

$$\dot{V}_n(t)\le-c\mu(t)\chi_1+n\mu(t)d\sigma(t)+\bar{\eta}, \tag{48}$$

where $\bar{\eta}=0.2785k_\gamma+\frac{1}{2}\beta_2\bar{W}^2+\frac{1}{2c_n}\|\varepsilon\|^2$ is positive. Then, by applying **Corollary 1**, one obtains $\lim_{t\to T_P^-}\chi_1(t)=0,$ and thus it is easy to obtain $\lim_{t\to T_P^-}\sum_{i=1}^{n}\xi_i^2=0.$ Together with the state transformation (18), this implies $\lim_{t\to T_P^-}(\xi_i,\mu(t)\lambda_i)=0,$ which means that, as $t\to T_P^-$, the variables λ_i converge to zero faster than $\mu(t)$ tends to infinity. Moreover, from the definition of the virtual controller α_1 in (24), it follows that $\lim_{t\to T_P^-}x_2(t)=0$. By repeating the same argument, one can further obtain $\lim_{t\to T_P^-}x_i(t)=0,i=3,\ldots,n$; then, by continuity, we finally have $\lim_{t\to T_p}x_i(t)=0,i=1,\ldots,n.$ Thus, the prescribed-time convergence is achieved. Since $V_n(t)$ is bounded on $[0,T_p)$, $\hat{d}(T_p)$ and $\widehat{W}(T_p)$ are finite. For

$t \geq T_p$, $\dot{\hat{d}} = 0$, and hence, $\hat{d}(t)$ remains bounded. Moreover, there exist positive constants c_p and η_p such that

$$\dot{V}_n(t) \leq -c_p \chi_1(t) - \frac{\beta}{2} \|\widetilde{W}\|^2 + \eta_p. \tag{49}$$

Defining

$$V_a = \chi_1 + \frac{1}{2\delta} \|\widetilde{W}\|^2 \tag{50}$$

and $\lambda_p = min\{c_p, \beta\delta\}$, one obtains

$$\dot{V}_a \leq -\lambda_p V_a + \eta_p. \tag{51}$$

Therefore, $\chi_1, \widetilde{W}, x_i$, and $\widehat{W}$ are uniformly ultimately bounded, and the system states remain within a bounded neighborhood of the origin after T_p.

To prove that the Zeno behavior does not occur under the event-triggered mechanism (39), define the inter-event interval as $t_k^* = t_{k+1} - t_k$. From (39), we have

$$E(t) = v(t) - u(t) = v(t) - v(t_k),\ \forall t \in [t_k, t_{k+1}). \tag{52}$$

Assume, for contradiction, that $t_k^* \to 0$. Then, from (52), it follows that

$$\lim_{t_k^* \to 0} |E(t_k + t_k^*)| = \lim_{t_k^* \to 0} |v(t_k + t_k^*) - v(t_k)| = 0. \tag{53}$$

However, from the triggering condition (39), we know

$$|E(t_{k+1})| \geq \omega_1 \, tanh|u(t)| + \omega_2 > 0. \tag{54}$$

From (54), we obtain $|E(t_k + t_k^*)| > 0$, which contradicts the result in (53). Therefore, the assumption does not hold, implying that Zeno behavior cannot occur. Furthermore, the positive lower bound of the inter-event interval can be explicitly derived as follows.

For $t \in [t_k, t_{k+1})$, according to the event-triggered controller, the actual input is held as

$$u(t) = v(t_k). \tag{55}$$

Thus, the event-triggering error can be rewritten as

$$E(t) = v(t) - u(t) = v(t) - v(t_k). \tag{56}$$

It is obvious that $E(t_k) = 0$. From the triggering condition (39), at the next triggering instant t_{k+1}, one has

$$|E(t_{k+1})| \geq \omega_1 \, tanh|u(t_{k+1}^-)| + \omega_2. \tag{57}$$

Since $tanh|u(t_{k+1}^-)| \geq 0$, it follows that

$$\omega_1 \, tanh|u(t_{k+1}^-)| + \omega_2 \geq \omega_2 > 0. \tag{58}$$

Therefore,

$$|E(t_{k+1})| \geq \omega_2. \tag{59}$$

On the other hand, since all closed-loop signals are bounded, and the continuous control signal $v(t)$ is smooth, there exists a positive constant L_v such that

$$|\dot{v}(t)| \leq L_v \tag{60}$$

on the considered finite time interval. Hence, for any $t \in [t_k, t_{k+1})$, we have

$$\begin{aligned} |E(t)| &= |v(t) - v(t_k)| \\ &\leq \left| \int_{t_k}^{t} \dot{v}(t) ds \right| \\ &\leq L_v(t - t_k). \end{aligned} \tag{61}$$

Taking $t = t_{k+1}$, one obtains

$$|E(t_{k+1})| \leq L_v(t_{k+1} - t_k). \tag{62}$$

Combining this inequality with $|E(t_{k+1})| \geq \omega_2$, it yields

$$\omega_2 \leq L_v(t_{k+1} - t_k). \tag{63}$$

Thus,

$$(t_{k+1} - t_k) \geq \frac{\omega_2}{L_v} > 0. \tag{64}$$

Therefore, the inter-event interval has a strictly positive lower bound, and Zeno behavior is rigorously excluded. This completes the proof.

Remark 3: In many prescribed-time control methods [24,25] based on robust compensation, the upper bound of external disturbances is typically required to be known in advance so that sufficiently large robust gains can be selected. However, this assumption is difficult to satisfy in practical systems and often leads to overly conservative control inputs. In this work, an RBFNN is employed to approximate the unknown disturbance online, and only the boundedness of the disturbance and approximation error is assumed. The explicit numerical value of the disturbance upper bound is not needed in the controller design. This avoids conservative prior estimation of disturbance bounds and allows the approximation error to be incorporated into the Lyapunov analysis in a unified manner, thereby ensuring that the closed-loop system maintains strong robustness while achieving prescribed-time convergence. [13] investigated prescribed-time stabilization of nonlinear systems with uncertainties and disturbances using an improved time-varying feedback approach. Building on this line of research, the present work further integrates adaptive compensation of unknown time-varying parametric uncertainties, RBFNN-based online disturbance compensation, and event-triggered implementation into a unified prescribed-time backstepping framework.

Remark 4: Compared with existing prescribed-time control results, the system considered in this paper involves a more comprehensive uncertainty structure. [8] investigated adaptive prescribed-time control for nonlinear systems with parametric uncertainties but did not consider event-triggered implementation or external disturbances. [20] addressed event-triggered prescribed-time stabilization with unknown time-varying parameters, but did not explicitly consider external disturbances. [25] considered disturbances, whereas parametric uncertainties are time-invariant. [26] also employed event-triggered communication to reduce unnecessary updates, but focused on cooperative control of multi-agent systems with unknown control directions. In contrast, this paper studies prescribed-time stabilization of strict-feedback nonlinear systems, where the adaptive law compensates for unknown time-varying parametric uncertainties and the RBFNN handles external disturbances. The main similarities and differences are summarized in Table 2.

Table 2. Comparison with representative existing control methods.

Method	Prescribed-time stabilization	Event-triggered implementation	Type of parametric uncertainty	External disturbances
Ref. [8]	√	×	Time-invariant	×
Ref. [20]	√	√	Time-varying	×
Ref. [24]	√	×	None	√
Ref. [25]	√	×	Time-invariant	√
Ref. [26]	×	√	Time-invariant	√
Proposed method	√	√	Time-varying	√

Remark 5: Compared with the fixed-threshold event-triggered mechanism in [27], the proposed triggering threshold satisfies $\omega_2 \leq \omega_1 \, tanh|u(t)| + \omega_2 \leq \omega_1 + \omega_2$. Therefore, the threshold increases with the magnitude of the control input, which allows a larger triggering error and may reduce unnecessary control updates, while it approaches ω_2 when the control input is small to maintain control accuracy. Moreover, the proposed triggering condition is analyzed jointly with the prescribed-time controller. The derived positive lower bound of the inter-event intervals excludes Zeno behavior and facilitates event-triggered implementation.

Remark 6: [28] developed an event-triggered prescribed-performance controller with a fixed threshold and a 1-bit actuator update protocol, guaranteeing that the tracking errors remain within predefined performance envelopes. [29] proposed a continuous PI funnel controller for unknown lower-triangular nonlinear systems, achieving prescribed tracking accuracy and attenuation of error oscillations. However, these methods focus on prescribed-performance tracking rather than prescribed-time stabilization, and the latter does not consider event-triggered implementation. In contrast, the proposed method addresses prescribed-time stabilization of strict-feedback nonlinear systems with unknown time-varying parameters and external disturbances under event-triggered implementation.

4. Simulation results

Example 1: To verify the effectiveness of the proposed control scheme, consider the following nonlinear system:

$$\begin{cases} \dot{x}_1 = x_2(t) + \theta_1(t) f_1(x_1), \\ \dot{x}_2 = u(t) + \theta_2(t) f_2(x_1, x_2) + w(t), \end{cases} \tag{65}$$

where the time-varying parameters, nonlinear functions, and external disturbance are chosen as

$$\begin{gathered} \theta_1(t) = 0.5\, sin(t), \ \ \theta_2(t) = 0.3\, cos(t), \\ f_1(x_1) = x_1^2, \ f_2(x_1, x_2) = x_2^2 + x_1, \ w = 0.5\, sin\, t\, . \end{gathered} \tag{66}$$

From (65) and (66), the upper-bound-related constant of the time-varying parametric uncertainties can be selected as

$$d = \sup_{t \geq 0} \|\theta_1(t), \theta_2(t)\| = 0.5. \tag{67}$$

It should be noted that d is not the exact value of the time-varying parameters, but an upper-bound-related constant used in the adaptive compensation design. To construct the RBFNN for disturbance approximation, $N = 101$ nodes are used in the simulation. The centers are uniformly distributed in the interval [-10,10], namely,

$$\varsigma_j = -10 + \frac{20(j-1)}{N-1}, j = 1, \dots, N. \tag{68}$$

The basis function vector is defined as

$$\Omega(x) = [\Omega_1(x), \Omega_2(x), \dots, \Omega_N(x)]^T, \Omega_j = exp\left[\frac{-(x-\varsigma_j)^T(x-\varsigma_j)}{\kappa_j^2}\right], j = 1, \dots, N. \tag{69}$$

The width is selected as $\kappa_j = 100, j = 1, \dots, N$. The interval [-10,10] is chosen to cover the main operating range of the RBFNN input during the simulation. Increasing the number of nodes can improve the approximation accuracy, but it also increases the computational cost. Therefore, $N = 101$ is selected as a tradeoff between approximation accuracy and implementation complexity.
The design parameters are chosen as

$$c_1 = 3, c_2 = 3, \sigma(t) = T_p - t, T_p = 5s, \varepsilon = 1, \omega_1 = 0.01, \omega_2 = 0.05, k_\gamma = 1, \beta = 0.01. \tag{70}$$

The initial conditions of the system are

$$(x_1(0), x_2(0)) = (1, -1). \tag{71}$$

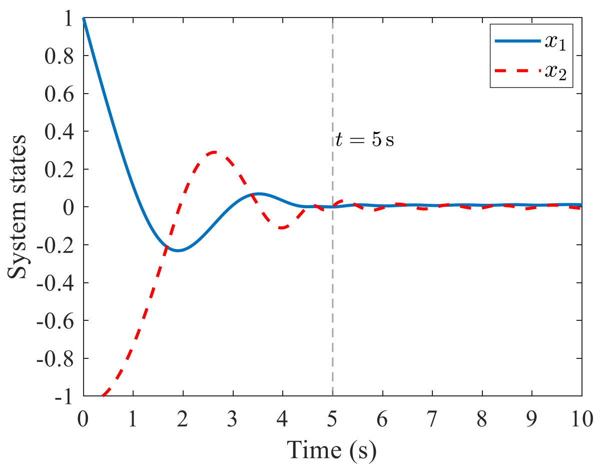

Figure 1. Response of system states.

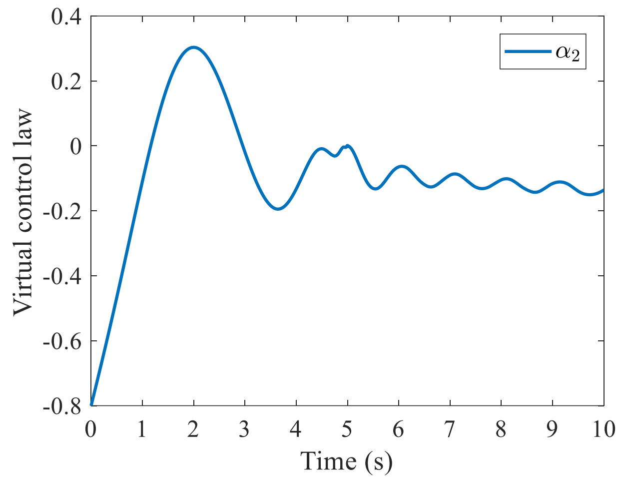

Figure 2. Response of α_2.

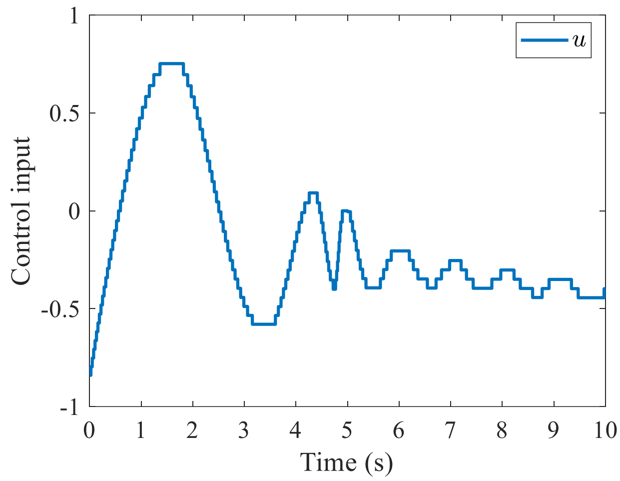

Figure 3. Response of u.

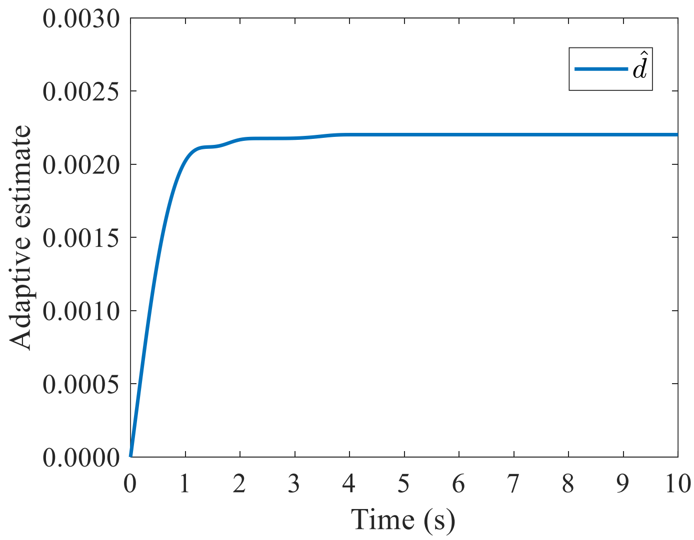

Figure 4. Response of $\hat{d}$.

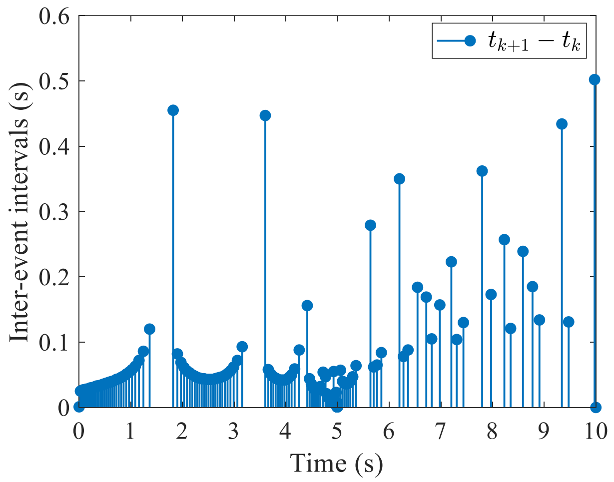

Figure 5. Response of inter-event intervals.

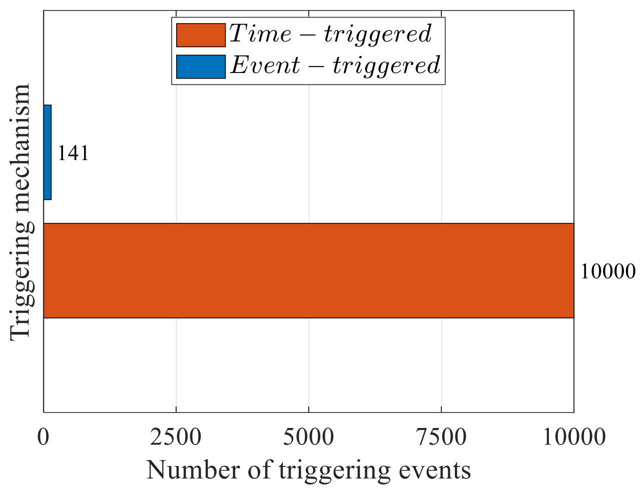

Figure 6. Comparison of triggering counts between the event-triggered strategy and the traditional time-triggered strategy.

The simulation results are shown in Figures 1–8. Figure 1 presents the responses of the system states. It can be observed that x_1 and x_2 converge to the origin before the prescribed time of 5 s and remain bounded after 5 s. This verifies the prescribed-time convergence and post-prescribed-time practical boundedness of the closed-loop system. Figures 2 and 3 show the continuous control signal α_2 and the actual event-triggered control input u, respectively. It can be seen that both signals remain bounded during the whole simulation. Figure 4 shows the response of the adaptive estimate $\hat{d}$, which remains bounded and tends to a steady value. Figure 5 gives the inter-event intervals, where all intervals are positive, indicating that Zeno behavior is excluded. Figure 6 compares the number of control updates between the time-triggered implementation and the proposed event-triggered mechanism. For a sampling period of 1 ms over 10 s, the time-triggered implementation generates 10,000 updates, whereas the proposed event-triggered mechanism triggers only 141 events, yielding a 98.59% reduction in control updates. These results demonstrate the effectiveness of the proposed event-triggered adaptive prescribed-time control strategy. In addition, Figures 7 and 8 show the state responses under two different external disturbances, namely $w(t) = 0.9\, sin(0.2t)$ and $w(t) = 0.2\, sin(0.2t)$, respectively. All the remaining controller parameters and initial conditions are kept unchanged. It can be observed that the system states still converge to the origin before the prescribed time, which further verifies the robustness of the proposed method against external disturbances.

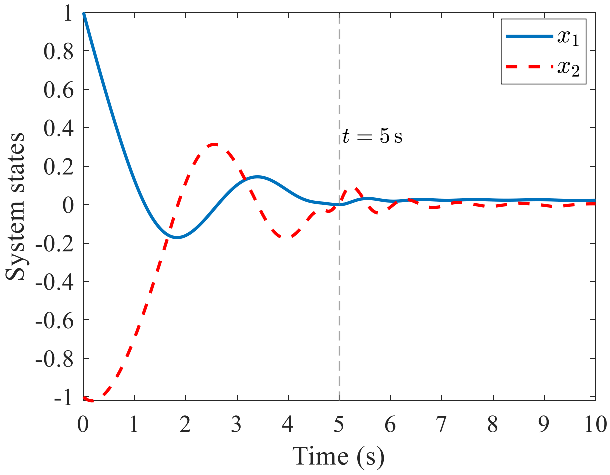

Figure 7. Response of system states under $w(t) = 0.9\, sin(0.2t)$.

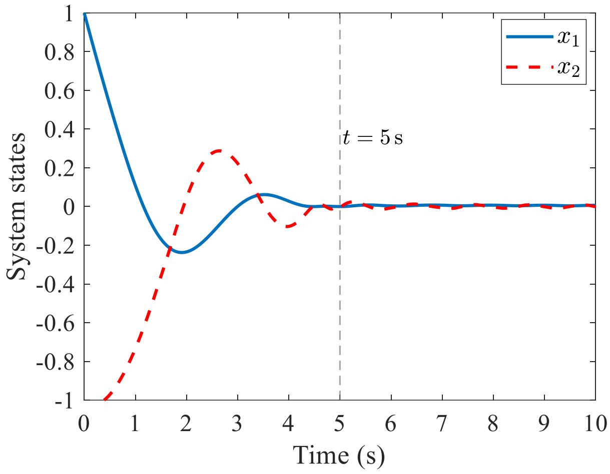

Figure 8. Response of system states under $w(t) = 0.2\, sin(0.2t)$.

Example 2: To further demonstrate the engineering applicability of the proposed method, an RLC circuit system with time-varying resistance is considered. The schematic diagram of the RLC circuit is shown in Figure 9. According to Kirchhoff's voltage law, the ideal RLC circuit model can be described as

$$LC\ddot{V}_c(t) + CR(t)\dot{V}_c(t) + V_c(t) = V_i(t), \tag{72}$$

where L denotes the inductance, C denotes the capacitance, $R(t)$ represents the resistance, which varies with temperature and humidity, V_i denotes the input voltage, and V_c denotes the voltage across the capacitor.

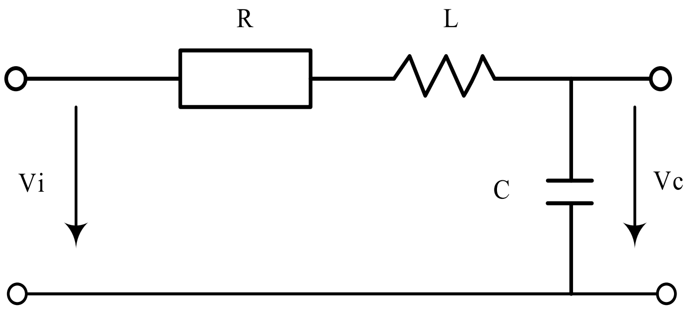

Figure 9. Schematic diagram of the RLC circuit.

Define the state variables as

$$x_1 = V_c, x_2 = \dot{V}_c, u = \frac{1}{LC} V_i, \tag{73}$$

then the system can be expressed as

$$\begin{cases} \dot{x}_1 = x_2(t) \\ \dot{x}_2 = u(t) + \theta(t) x_2 - \frac{1}{LC} x_1 \end{cases}, \tag{74}$$

where $\theta(t) = -\frac{R(t)}{L}$ is the time-varying parameter.

To describe the dynamic behavior of the practical RLC circuit system more accurately under complex operating conditions, external disturbances, modeling errors, and unmodeled dynamics are further considered. Based on the original system model, the disturbance term $w(t)$ is introduced, and the following extended state-space model is obtained:

$$\begin{cases} \dot{x}_1 = x_2(t) \\ \dot{x}_2 = u(t) + \theta(t) x_2 - \frac{1}{LC} x_1 + w(t). \end{cases} \tag{75}$$

The prescribed time is selected as 8 s. The system parameters and disturbance function are chosen as

$$L = 10\, H, C = 100\, mF, R(t) = 50 + 5\, cos(t)\, \Omega, w(t) = 0.1\, sin(t). \tag{76}$$

Therefore, one obtains

$$\theta(t) = -\frac{R(t)}{L} = -5 - 0.5\, cos(t). \tag{77}$$

Thus, the unknown time-varying parameter satisfies

$$d = \sup_{t \geq 0} |\theta(t)| = 5.5. \tag{78}$$

The initial conditions of the system are selected as

$$\big(x_1(0), x_2(0)\big) = (5{,}5). \tag{79}$$

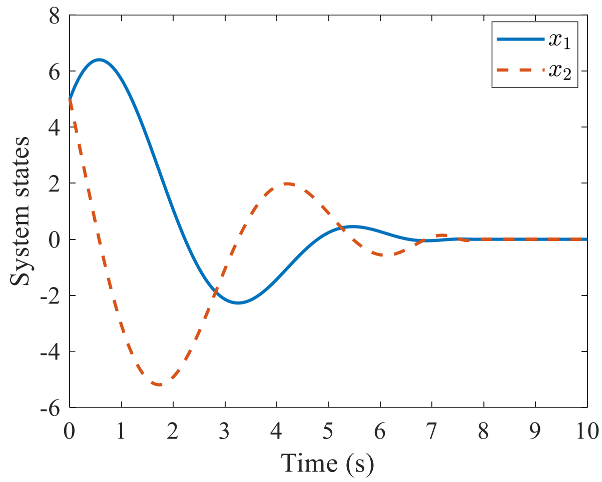

Figure 10. Response of system states.

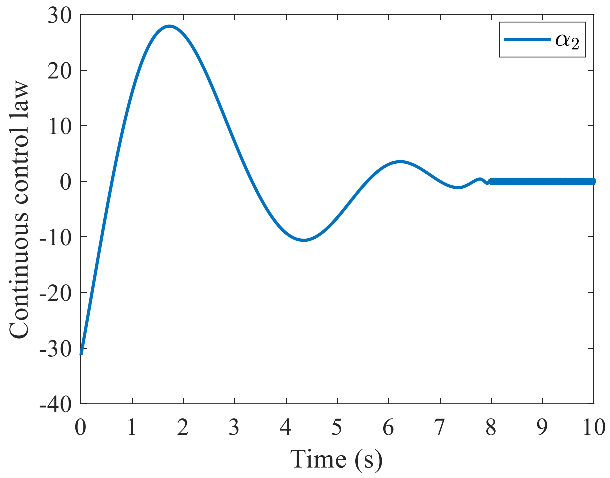

Figure 11. Response of α_2.

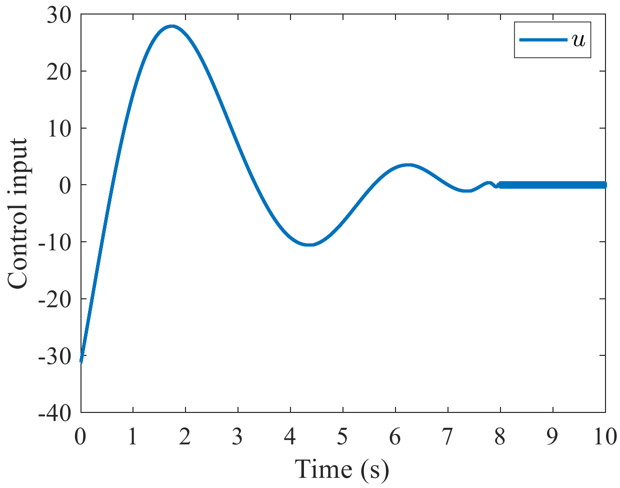

Figure 12. Response of u.

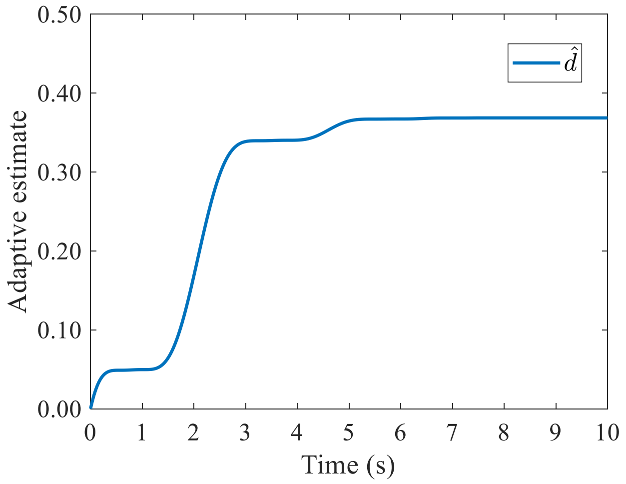

Figure 13. Response of $\hat{d}$.

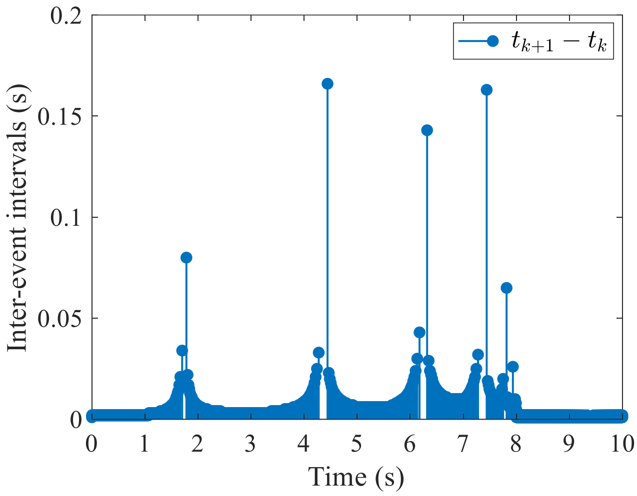

Figure 14. Response of inter-event intervals.

The simulation results are shown in Figures 10–14. Figure 10 shows that the system states x_1 and x_2 converge to the origin before the prescribed time of 8 s and remain bounded after 8 s. Figures 11 and 12 present the continuous control signal α_2 and the actual control input u, respectively. It can be seen that both signals remain bounded during the whole simulation. Figure 13 shows that the adaptive estimate $\hat{d}$ is bounded, which indicates that the adaptive law can compensate for the unknown time-varying uncertainty. Figure 14 gives the inter-event intervals, where all intervals are positive, showing that Zeno behavior is excluded. Therefore, the proposed method is effective for the RLC circuit system with time-varying resistance and external disturbance.

5. Conclusions

In this work, the event-triggered control problem for a class of nonlinear systems with external disturbances and uncertain time-varying parameters has been successfully addressed. First, by incorporating a structurally simple prescribed-time adjustment function into the backstepping design, the structural complexity of recursive construction is effectively reduced. Second, by embedding a radial basis function neural network into the controller, the influence of unknown external disturbances is compensated online. Finally, an event-triggered mechanism is incorporated and co-designed with the controller, ensuring prescribed-time stability while significantly reducing the number of triggering events compared with conventional time-triggered strategies, thus saving communication and computational resources. It should be noted that the unified upper-bound estimate adopted in this work may introduce additional transient conservatism when the uncertainty levels of different subsystems differ significantly. In future research, individual adaptive estimates will be designed for the time-varying parametric uncertainties at different backstepping steps to further reduce this conservatism and improve transient control performance.

Use of AI tools declaration

During the preparation of this work, the authors used an AI language model (ChatGPT) solely for language polishing. No AI tools were used to generate research ideas, data, analysis, or scientific conclusions. The authors have reviewed and taken full responsibility for the final content of this article.

Acknowledgments

This work was supported by the Humanities and Social Science Fund of the Ministry of Education of China (No. 23YJAZH031), the Natural Science Foundation of Hebei Province of China (No. A2023209002), the Tangshan Science and Technology Bureau Program of Hebei Province of China (No. 24130201C), the Fundamental Research Funds for Hebei Province Universities (North China University of Science and Technology) (No. JJC2024045), the Graduate Student Innovation Fund of North China University of Science and Technology (No. 2025S01), the Yanzhao Iron and Steel Laboratory Regional Innovation Capacity Improvement Project (No. YZISL2024014), and the Tangshan Talent Funding Program (No. B202302009).

Conflict of interest

The authors declare there are no conflict of interest.

References

1. W. M. Haddad, A. L'Afflitto, Finite-time stabilization and optimal feedback control, *IEEE Trans. Autom. Control*, **61** (2016), 1069–1074. https://doi.org/10.1109/TAC.2015.2454891
2. A. Polyakov, Nonlinear feedback design for fixed-time stabilization of linear control systems, *IEEE Trans. Autom. Control*, **57** (2012), 2106–2110. https://doi.org/10.1109/TAC.2011.2179869
3. Y. D. Song, Y. Wang, J. Holloway, M. Krstic, Time-varying feedback for regulation of normal-form nonlinear systems in prescribed finite time, *Automatica*, **83** (2017), 243–251. https://doi.org/10.1016/j.automatica.2017.06.008
4. Y. Wang, Y. Song, A general approach to precise tracking of nonlinear systems subject to non-vanishing uncertainties, *Automatica*, **106** (2019), 306–314. https://doi.org/10.1016/j.automatica.2019.05.008

5. F. Gao, Y. Wu, Z. Zhang, Global fixed-time stabilization of switched nonlinear systems: A time-varying scaling transformation approach, *IEEE Trans. Circuits Syst. II Express Briefs*, **66** (2019), 1890–1894. https://doi.org/10.1109/TCSII.2018.2890556
6. Y. D. Song, H. F. Ye, F. L. Lewis, Prescribed-time control and its latest developments, *IEEE Trans. Syst. Man Cybern.: Syst.*, **53** (2023), 4102–4116. https://doi.org/10.1109/TSMC.2023.3240751
7. B. Zhou, Y. Shi, Prescribed-time stabilization of a class of nonlinear systems by linear time-varying feedback, *IEEE Trans. Autom. Control*, **66** (2021), 6123–6130. https://doi.org/10.1109/TAC.2021.3061645
8. C. C. Hua, P. Ning, K. Li, Adaptive prescribed-time control for a class of uncertain nonlinear systems, *IEEE Trans. Autom. Control*, **67** (2022), 6159–6166. https://doi.org/10.1109/TAC.2021.3130883
9. P. J. Ning, C. C. Hua, K. Li, H. Li, A novel theorem for prescribed-time control of nonlinear uncertain time-delay systems, *Automatica*, **152** (2023), 111009. https://doi.org/10.1016/j.automatica.2023.111009
10. B. Liu, J. Li, R. C. Ma, J. Fu, Adaptive prescribed-time tracking control for uncertain nonlinear systems with full state constraints, *Int. J. Adapt. Control Signal Process.*, **38** (2024), 1262–1280. https://doi.org/10.1002/acs.3744
11. Y. Zhang, M. Chadli, Z. Xiang, Prescribed-time adaptive fuzzy optimal control for nonlinear systems, *IEEE Trans. Fuzzy Syst.*, **32** (2024), 2403–2412. https://doi.org/10.1109/TFUZZ.2024.3352590
12. Y. Zhang, M. Chadli, Z. Xiang, Predefined-time adaptive fuzzy control for a class of nonlinear systems with output hysteresis, *IEEE Trans. Fuzzy Syst.*, **31** (2023), 2522–2531. https://doi.org/10.1109/TFUZZ.2022.3228012
13. L. C. Feng, M. Y. Dai, N. Ji, Y. L. Zhang, L. P. Du, Prescribed-time stabilization of nonlinear systems with uncertainties/disturbances by improved time-varying feedback control, *AIMS Math.*, **9** (2024), 23859–23877. https://doi.org/10.3934/math.20241159
14. C. C. Li, C. Y. Zhang, L. C. Feng, Z. H. Wu, Note on prescribed-time stability of impulsive piecewise-smooth differential systems and application in networks, *Networks Heterogen. Media*, **19** (2024), 970–991. https://doi.org/10.3934/nhm.2024043
15. L. C. Feng, C. C. Li, M. Abdel-Aty, J. D. Cao, Prescribed-time stability of nonlinear impulsive piecewise systems and synchronization for dynamical networks, *Qual. Theory Dyn. Syst.*, **24** (2025), 165. https://doi.org/10.1007/s12346-025-01302-1
16. F. L. Lewis, S. Jagannathan, A. Yesildirak, *Neural Network Control of Robot Manipulators and Nonlinear Systems*, London: Taylor & Francis, 1999.
17. M. Li, S. Li, C. K. Ahn, Z. Xiang, Adaptive fuzzy event-triggered command-filtered control for nonlinear time-delay systems, *IEEE Trans. Fuzzy Syst.*, **30** (2022), 1025–1035. https://doi.org/10.1109/TFUZZ.2021.3052095
18. S. Li, C. K. Ahn, J. Guo, Z. Xiang, Neural-network approximation-based adaptive periodic event-triggered output-feedback control of switched nonlinear systems, *IEEE Trans. Cybern.*, **51** (2021), 4011–4020. https://doi.org/10.1109/TCYB.2020.3022270
19. P. J. Ning, C. C. Hua, K. Li, R. Meng, Event-triggered control for nonlinear uncertain systems via a prescribed-time approach, *IEEE Trans. Autom. Control*, **68** (2023), 6975–6981. https://doi.org/10.1109/TAC.2023.3243863

20. P. J. Ning, C. C. Hua, K. Li, R. Meng, Event-triggered adaptive prescribed-time control for nonlinear systems with uncertain time-varying parameters, *Automatica*, **157** (2023), 111229. https://doi.org/10.1016/j.automatica.2023.111229
21. W. Sun, J. Zhao, W. Sun, J. Xia, Z. Sun, Adaptive event-triggered global fast finite-time control for a class of uncertain nonlinear systems, *Int. J. Robust Nonlinear Control*, **30** (2020), 3773–3785. https://doi.org/10.1002/rnc.4966
22. K. Li, C. C. Hua, X. You, X. Guan, Output feedback-based consensus control for nonlinear time-delay multiagent systems, *Automatica*, **111** (2020), 108669. https://doi.org/10.1016/j.automatica.2019.108669
23. J. Du, X. Hu, M. Krstic, Y. Sun, Robust dynamic positioning of ships with disturbances under input saturation, *Automatica*, **73** (2016), 207–214. https://doi.org/10.1016/j.automatica.2016.06.020
24. L. C. Feng, C. L. Zhang, M. Abdel-Aty, J. D. Cao, F. E. Alsaadi, Prescribed-time trajectory tracking control for a class of nonlinear system, *Electron. Res. Arch.*, **32** (2024), 6535–6552. https://doi.org/10.3934/era.2024305
25. L. T. Zhou, L. C. Feng, N. Ji, R. C. Zhang, Backstepping-sliding-mode-based prescribed-time control for a class of nonlinear systems with disturbances, *AIMS Math.*, **10** (2025), 22791–22816. https://doi.org/10.3934/math.20251013
26. Y. W. Wang, Y. Lei, T. Bian, Z. H. Guan, Distributed control of nonlinear multiagent systems with unknown and nonidentical control directions via event-triggered communication, *IEEE Trans. Cybern.*, **50** (2020), 1820–1832. https://doi.org/10.1109/TCYB.2019.2908874
27. Z. Li, J. Yan, W. Yu, J. Qiu, Adaptive event-triggered control for unknown second-order nonlinear multiagent systems, *IEEE Trans. Cybern.*, **51** (2021), 6131–6140. https://doi.org/10.1109/TCYB.2020.2964430
28. J. X. Zhang, G. H. Yang, Event-triggered prescribed performance control for a class of unknown nonlinear systems, *IEEE Trans. Syst., Man, Cybern.: Syst.*, **51** (2021), 6576–6586. https://doi.org/10.1109/TSMC.2019.2963215
29. J. X. Zhang, T. Chai, Proportional-integral funnel control of unknown lower-triangular nonlinear systems, *IEEE Trans. Autom. Control*, **69** (2024), 1921–1927. https://doi.org/10.1109/TAC.2023.3330900